Numerical method for calculating the dynamic behaviour of a trolley wire overhead contact system for electric railways

M. R. Abbott

Mathematics Department, Royal Aircraft Establishment, Farnborough, Hampshire

A numerical method is described that has been used for predicting the dynamic behaviour of a trolley wire overhead contact system when disturbed by the pantograph on the train roof. The vertical motion of the trolley wire is given by the solution of a fourth order partial differential equation and that of the pantograph is given by the solution of ordinary differential equations, these two solutions being linked by the conditions holding at the contact point. Results obtained from the method have encouraged British Rail to set up a test line of this equipment to see if a trolley wire can be developed as a cheap alternative to the present more elaborate systems.

(Received September 1969)

The simplest and cheapest type of overhead system is the trolley wire, in which the contact wire is suspended directly from springs at widely spaced intervals λ, the span length. The system is depicted diagrammatically in **Fig. 1**. In the more complicated systems in present use the contact wire is attached by droppers at frequent intervals to a catenary wire; only the catenary wire is attached at the supports and the contact wire is approximately horizontal, the structure resembling a series of suspension bridges.

Mathematical model of a trolley wire system

The contact wire is assumed to behave as a thin heavy beam under tension. The contact force P acts vertically and travels along the wire at the constant train speed u; this force is variable and is to be determined. The maximum value of the contact force occurs near the supports and a design of the system is required which keeps the maximum force down to a reasonable level, and at the same time keeps the contact force at intermediate positions above zero, to avoid separation between the head of the pantograph and the wire. In this work contact is assumed at all times, so that if separation occurs it is shown by P becoming negative. However, this has not occurred in any examples.

The vertical motion of the wire is described by the equation

$$\rho\frac{\partial^2 y}{\partial t^2} + EI\frac{\partial^4 y}{\partial x^4} - T\frac{\partial^2 y}{\partial x^2} + \mu\frac{\partial y}{\partial t} + S\sum_r y\delta(x - r\lambda) = P(t)\delta(x - ut - \tfrac{1}{2}\lambda). \quad (1)$$

The dependent variable $y(x, t)$ is the upward vertical displacement of the wire measured from the undisturbed equilibrium position, taken here as $y = y_0(x)$. The variable x is the along-track coordinate and t is the time. The quantities ρ, EI and T are the linear density, flexural rigidity and tension of the wire respectively, μ is a damping coefficient, S the spring constant of the supporting springs, and $P(t)$ the contact force acting at the point $x = ut + \frac{1}{2}\lambda$. This equation is in terms of vertical forces per unit length of the wire, so that forces acting at a point are represented by delta functions. The shear force is discontinuous at the contact point $x = ut + \frac{1}{2}\lambda$ and at each of the supports $x = r\lambda$, $r = 0, 1, \ldots, m$. Equation (1) is partly hyperbolic and partly parabolic, or in other words the propagation of disturbances along the wire is partly by wave motion and partly by diffusion. The origin of x is taken at a support position, with the contact point at a mid-span position $x = \frac{1}{2}\lambda$ at $t = 0$; this starting position, together with the assumed initial conditions given below, is found in numerical tests to produce very small transients, the required steady forced oscillation occurring very quickly. The contact point is taken half a span length from the end $x = 0$ at $t = 0$ and the motion is calculated until the contact point is about one-and-a-half span lengths from the other end of the wire at $x = m\lambda$. Numerical tests show that taking $m = 6$ gives results that are a close approximation to those for a very long length of wire.

The pantograph is represented by the system shown in **Fig. 1**. The vertical motion satisfies the equations

$$m_1\frac{d^2Y}{dt^2} + \mu_1\left(\frac{dY}{dt} - \frac{d\eta}{dt}\right) + k_1(Y - \eta) + P(t) + m_1 g = 0 \quad (2)$$

and

$$m_2\frac{d^2\eta}{dt^2} + \mu_2\frac{d\eta}{dt} = G + \mu_1\left(\frac{dY}{dt} - \frac{d\eta}{dt}\right) + k_1(Y - \eta) - m_2 g, \quad (3)$$

where Y and η are the vertical displacements of the pantograph head and frame, respectively; m_1 is the mass of the pantograph head and m_2 that of the frame; μ_1 is the damping coefficient for the motion of the head relative to the frame and μ_2 that for the frame motion,

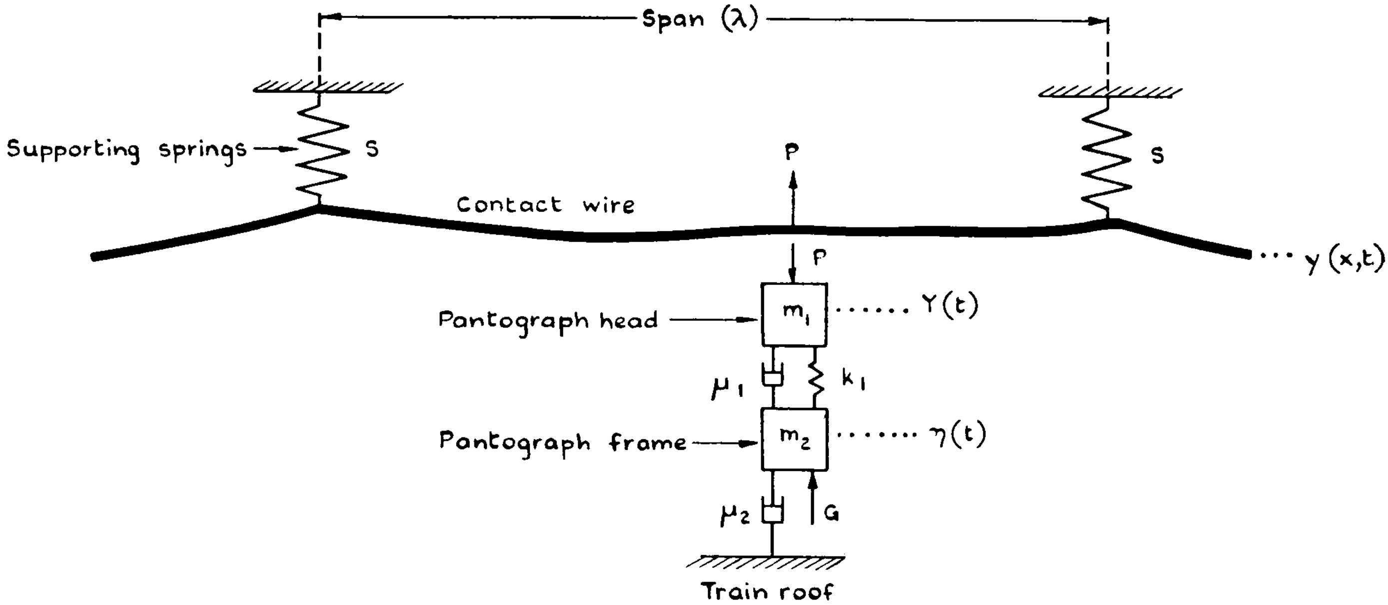

Fig. 1. Diagrammatic representation of trolley wire system and pantograph

it being assumed here that any vertical motion of the train roof can be neglected; k_1 is the constant for the spring between the head and the frame; P is the force exerted downwards on the pantograph head by the contact wire and G is the constant force acting on the frame from springs on the train roof. The vertical displacement of the pantograph head is measured from the horizontal line defined by the undisturbed wire level at the supports. The displacement of the wire from this datum is given by the solution $y(x, t)$ of (1), plus the equilibrium displacement $y_0(x)$. The variation of the latter quantity over a span is given by the solution of

$$EI\frac{d^4y_0}{dx^4} - T\frac{d^2y_0}{dx^2} + \rho g = 0, \tag{4}$$

having $y_0 = \frac{dy_0}{dx} = 0$ at the supports. For numerical values of current interest it can be shown that the solution of (4) at points more than a few feet away from a support is approximately

$$y_0 = -\frac{\rho g \xi}{2T}(\lambda - \xi) + \frac{\rho g \lambda}{2T}\left(\frac{EI}{T}\right)^{\frac{1}{2}} \tag{5}$$

where ξ is the distance from an adjacent support. But at the supports $y_0 = 0$, in agreement with the boundary condition. Thus, y_0 is given by the parabolic approximation for a perfectly flexible wire with small slope plus, at points more than a foot or so from the supports, a small constant upward displacement given by the last term of (5). This displacement has the effect of reducing the sharpness of the profile change at the supports. If the finite difference space step Δx in the numerical solution described below is taken very small, a more accurate determination of $y_0(x)$ is necessary in the vicinity of the supports.

The contact condition to be satisfied by the solutions of the contact wire equation and the pantograph equations is

$$y(\tfrac{1}{2}\lambda + ut, t) + y_0(\tfrac{1}{2}\lambda + ut) = Y(t). \tag{6}$$

The initial conditions are taken as $P = 0$ with no vertical motion of the pantograph and the wire at rest in the equilibrium position, so that $Y(0) = y_0(\frac{1}{2}\lambda)$. The motion is started by applying a step change of G at $t = 0$ from $G = (m_1 + m_2)g$, i.e. just sufficient to balance the weight of the pantograph, to $G = (m_1 + m_2)g + P_*$, where P_* is a constant force. The effect of this step change is transmitted to the wire through the two parts of the pantograph. The wire oscillates and the contact force varies as the pantograph travels along the wire, and the behaviour of Y and P in the eventual steady oscillation is the important result for assessing the performance.

Outline of method of solution

The solution is obtained by numerical integration of (1), (2) and (3) through time steps Δt, using the following sequence of operations at each new pivotal value of t:

(*a*) assume $P(t) = P(t - \Delta t)$;

(*b*) obtain the numerical solution of the wire equation (1) at time t for the assumed value of $P(t)$;

(*c*) obtain the solution of the pantograph equations at time t for the assumed value of $P(t)$ [this calculation is completely independent of step (*b*) except for using the same value of $P(t)$]—the contact condition will not be satisfied;

(*d*) change $P(t)$ to $P(t) + 1$ lbf and repeat steps (*b*) and (*c*)—again the contact condition will not be satisfied;

(*e*) from the results of these two trial solutions obtain by linear interpolation or extrapolation a third and final value of $P(t)$ which satisfies the contact condition (6) exactly;

(*f*) repeat steps (*b*) and (*c*) to obtain the required solution at time t.

The solution can then be found at time $t + \Delta t$, and so on, through as many time steps as required.

Step (*b*) is described in the following section. Step (*c*) uses the trapezium rule to integrate (2) and (3) from $t - \Delta t$ to t; this is straightforward. Step (*e*) makes use of the two values of the separation

$$y(\tfrac{1}{2}\lambda + ut, t) + y_0(\tfrac{1}{2}\lambda + ut) - Y(t)$$

found in the trial solutions for the two assumed values of $P(t)$, and depends on the fact that this separation is a linear function of P as the system is linear.

Numerical solution of the partial differential equation

Between adjacent supports or, in the span acted on by the pantograph, between the contact point and the neighbouring supports, the vertical motion of the wire is given by

$$\rho\frac{\partial^2 y}{\partial t^2} + EI\frac{\partial^4 y}{\partial x^4} - T\frac{\partial^2 y}{\partial x^2} + \mu\frac{\partial y}{\partial t} = 0. \qquad (7)$$

A fully-implicit method with backward t-differences permits the point forces at the supports and the contact point to be included very simply. Part of the x, t plane is shown in **Fig. 2**: $n + 1$ pivotal points are introduced in the x-direction, labelled from 0 to n and Δx apart, in such a way that supports occur at pivotal points. The finite difference solution y_i, $i = 0(1)n$, at time t is to be determined from the already computed solution at time $t - \Delta t$, a_i say, and from that at time $t - 2\Delta t$, b_i say. The finite difference steps are chosen to satisfy

$$\Delta x = u\Delta t, \qquad (8)$$

to ensure that the contact point always coincides with a pivotal point.

We consider first the finite difference equations at points neither at nor adjacent to the point forces. The fully-implicit finite difference approximation of (7) is taken as

$$\rho\left\{\frac{y_i - 2a_i + b_i}{(\Delta t)^2}\right\} + EI\left\{\frac{y_{i+2} - 4y_{i+1} + 6y_i - 4y_{i-1} + y_{i-2}}{(\Delta x)^4}\right\} - T\left\{\frac{y_{i+1} - 2y_i + y_{i-1}}{(\Delta x)^2}\right\} + \mu\left\{\frac{y_i - a_i}{\Delta t}\right\} = 0, \quad (9)$$

analogous to the fully-implicit finite difference representation of the one-dimensional heat flow equation. This equation in general relates five unknown values of y_i, and can be written for brevity as

$$c_0 y_{i-2} + c_1 y_{i-1} + c_2 y_i + c_1 y_{i+1} + c_0 y_{i+2} = fa_i + f'b_i = d_i, \text{ say.} \qquad (10)$$

The constants c_0, c_1, c_2, f and f' depend on the coefficients of (9) and the quantity d_i depends also on the previous solutions a_i and b_i.

This fully-implicit finite difference scheme can be proved to be unconditionally stable by substituting $\exp(\sqrt{-1}\kappa x)\xi^j$, where $t = j\Delta t$, for y_i, a_i and b_i in (9). (We write $\sqrt{-1}$ to avoid confusion with the use of i as the subscript in y_i, etc.) This substitution leads to a quadratic for ξ and it can be shown that $|\xi| < 1$ for all values of the ratio $\Delta x : \Delta t$.

An alternative scheme with reduced truncation error uses central t-differences and represents $\partial^4 y/\partial x^4$ and $\partial^2 y/\partial x^2$ in terms of the a's. But this method is not stable for a sufficiently wide range of $\Delta x : \Delta t$. In view of (8) it is important to have a method that is free of stability restrictions.

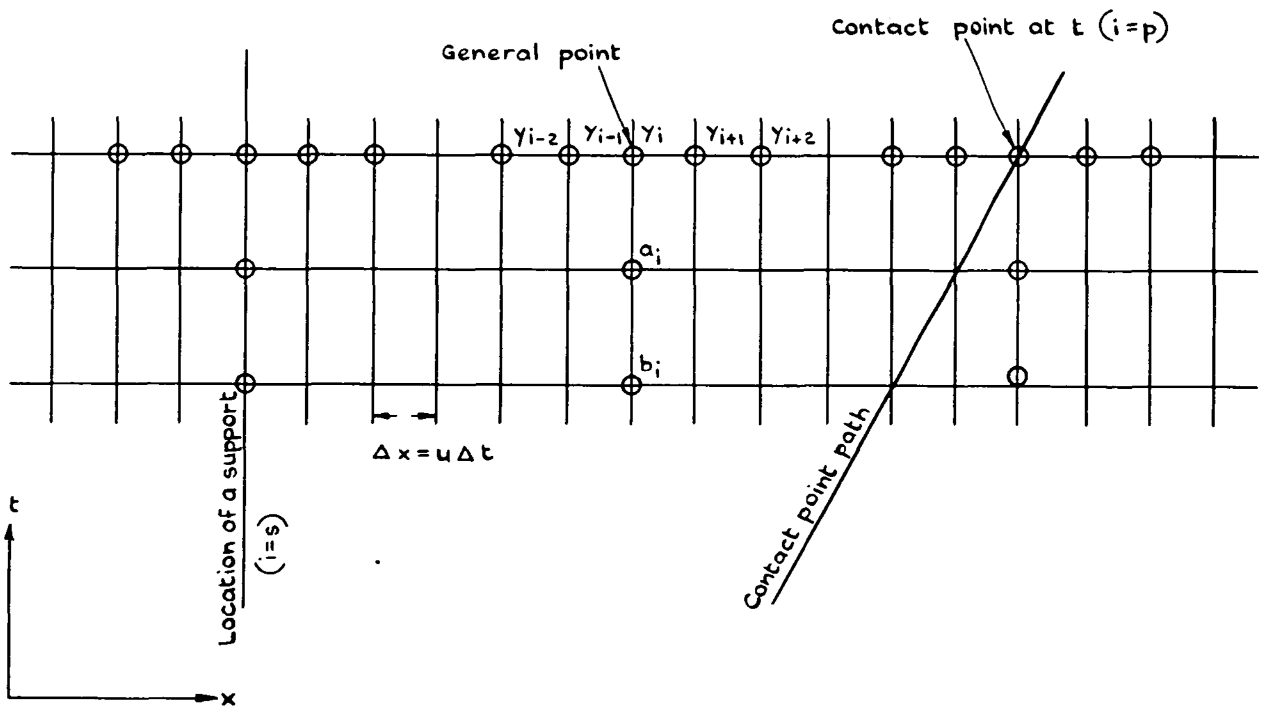

Fig. 2. ***x*, *t* plane**

A third possible scheme, resembling the Crank-Nicolson method for the one-dimensional heat flow equation, represents $\partial^4 y/\partial x^4$ and $\partial^2 y/\partial x^2$ as the mean of the finite difference approximations at t and $t - 2\Delta t$, that is in terms of the y's and b's, respectively. But this method leads to difficulties when considering the effects of the point forces, and is discarded in favour of the fully-implicit representation.

The next step is to take account of the contact and support forces. At the points of application of these:

$$y, \frac{\partial y}{\partial x} \text{ and } \frac{\partial^2 y}{\partial x^2} \text{ are continuous,} \tag{11}$$

and the discontinuity in shear force satisfies

$$\left.\begin{aligned} EI\left[\frac{\partial^3 y}{\partial x^3}\right] &= -Sy \text{ at a support,} \\ &= P \text{ at the contact point,} \\ &= P - Sy \text{ at the contact point when} \\ &\qquad \text{it coincides with a support.} \end{aligned}\right\} \tag{12}$$

Consider first a support, $i = s$, not coinciding with the contact point, $i = p$. Fictitious values of y_i are introduced: y^*_{s+1}, y^*_{s+2} associated with the solution in $x \lesssim s\Delta x$ and y^*_{s-2}, y^*_{s-1} associated with the solution in $x \gtrsim s\Delta x$; see **Fig. 3**. The fictitious values are obtained

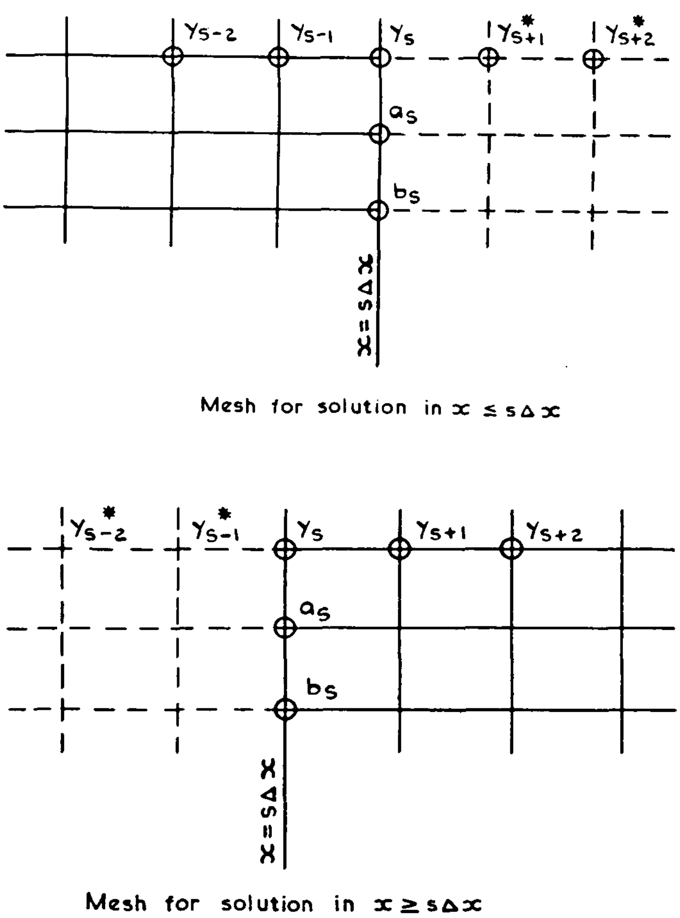

Fig. 3. Mesh points and values in finite difference formulae at $i = s$. Fictitious values are starred

from the finite difference expressions for the internal boundary conditions (11) and (12). In fact, the continuity of $\partial y/\partial x$ and $\partial^2 y/\partial x^2$, expressed by the 3-point formulae

$$y_{s+1} - y^*_{s-1} = y^*_{s+1} - y_{s-1}$$

and

$$y_{s+1} - 2y_s + y^*_{s-1} = y^*_{s+1} - 2y_s + y_{s-1},$$

gives
$$y^*_{s+1} = y_{s+1} \text{ and } y^*_{s-1} = y_{s-1}. \tag{13}$$

The first condition of (11) has been taken into account by using the common symbol y_s. Hence, points $i = s - 1$, $s + 1$ adjacent to a support contribute an equation conforming to the general form (10), in all respects. At a support position $i = s$ we have for the solution at $x = s\Delta x-$, that is just behind the contact point,

$$c_0 y_{s-2} + c_1 y_{s-1} + c_2 y_s + c_1 y_{s+1} + c_0 y^*_{s+2} = d_s, \tag{14}$$

and for the solution at $x = s\Delta x+$, that is just ahead of the contact point,

$$c_0 y^*_{s-2} + c_1 y_{s-1} + c_2 y_s + c_1 y_{s+1} + c_0 y_{s+2} = d_s. \tag{15}$$

Also, the first condition of (12), using the 5-point formula for $\partial^3 y/\partial x^3$ on each side of the discontinuity at $i = s$, gives

$$EI\left\{\left(\frac{2y_{s+2} - 4y_{s+1} + 4y_{s-1} - 2y^*_{s-2}}{4(\Delta x)^3}\right) - \left(\frac{2y^*_{s+2} - 4y_{s+1} + 4y_{s-1} - 2y_{s-2}}{4(\Delta x)^3}\right)\right\} = -Sy_s,$$

or

$$y_{s-2} + y_{s+2} - y^*_{s-2} - y^*_{s+2} = 2c(-Sy_s) \tag{16}$$

where

$$c = (\Delta x)^3/EI. \tag{17}$$

Multiplying (16) by c_0 and adding to the sum of (14) and (15) enables us to eliminate the remaining fictitious values, obtaining

$$c_0 y_{s-2} + c_1 y_{s-1} + (c_2 + cc_0 S)y_s + c_1 y_{s+1} + c_0 y_{s+2} = d_s. \tag{18}$$

Therefore the effect of each support is to add a term $cc_0 S$ to the coefficient of y_s in the relevant finite difference equation.

Similarly, at the contact point $i = p$ relations (13) to (17) hold with s replaced by p and the right-hand side of (16) replaced by $2cP(t)$. Hence the finite difference equation at the contact point is

$$\begin{aligned} c_0 y_{p-2} + c_1 y_{p-1} + c_2 y_p + c_1 y_{p+1} + c_0 y_{p+2} &= fa_p + f'b_p + cc_0 P(t), \\ &= d_p, \text{ say.} \end{aligned} \tag{19}$$

Therefore the effect of the contact force is to add a term $cc_0 P$ to the right side of the basic equation (10) for this one point. At time $t + \Delta t$ the following equation is the one modified in this way, and so on.

Further, by virtue of (13), it can be verified that these effects continue to apply when the contact point coincides with or is adjacent to a support. The point forces are thus taken account of very simply. In fact it can be shown from the values of the c's that the finite difference approximations used above are equivalent to spreading the point forces P and $-Sy$ over one space step Δx, so that there is a distributed force $P/\Delta x$ per unit length of the wire over a total length Δx from $p\Delta x - \frac{1}{2}\Delta x$ to $p\Delta x + \frac{1}{2}\Delta x$; and similarly for the spring forces at the supports.

The $n + 1$ finite difference equations can be written

$$Cy = d \tag{20}$$

at each value of t, where y is the column vector of the required finite difference solution and d is the column vector formed by the known values of the d_i. The end conditions are taken as

$$y_{-2} = y_{-1} = y_{n+1} = y_{n+2} = 0. \tag{21}$$

The matrix C is symmetric and quin-diagonal, the non-zero elements in each row are in general

$$c_0, c_1, c_2, c_1, c_0;$$

but for a pivotal point coinciding with a support (e.g. every 36th) the non-zero elements in the row are

$$c_0, c_1, c_2 + cc_0S, c_1, c_0.$$

There are obvious differences in the first two and final two rows of C. In practice the order of C may be many hundred.

Equation (20) is solved by factorising C into a lower triangular matrix L and an upper triangular matrix U, each having three non-zero diagonals. Since C is independent of t this factorisation is only required at the start of a calculation, the elements of L and U being stored; this permits the solution of (20) to be obtained quickly at each pivotal value of t for the various values of P.

In summary, the method of this section gives the finite difference solution of the wire equation at time t for a specified contact force. Two trial solutions and a final solution are required at each pivotal value of t.

Application and extensions

About forty examples have been computed for British Rail, to examine the effects of changing the various parameters of the wire and pantograph at selected train speeds. These preliminary results were encouraging and British Rail have taken over the computer program and examined further cases as well as setting up a full scale test line of this equipment. This account concentrates on the basic numerical method, and just one example is given in **Fig. 4**. This shows how quickly the steady

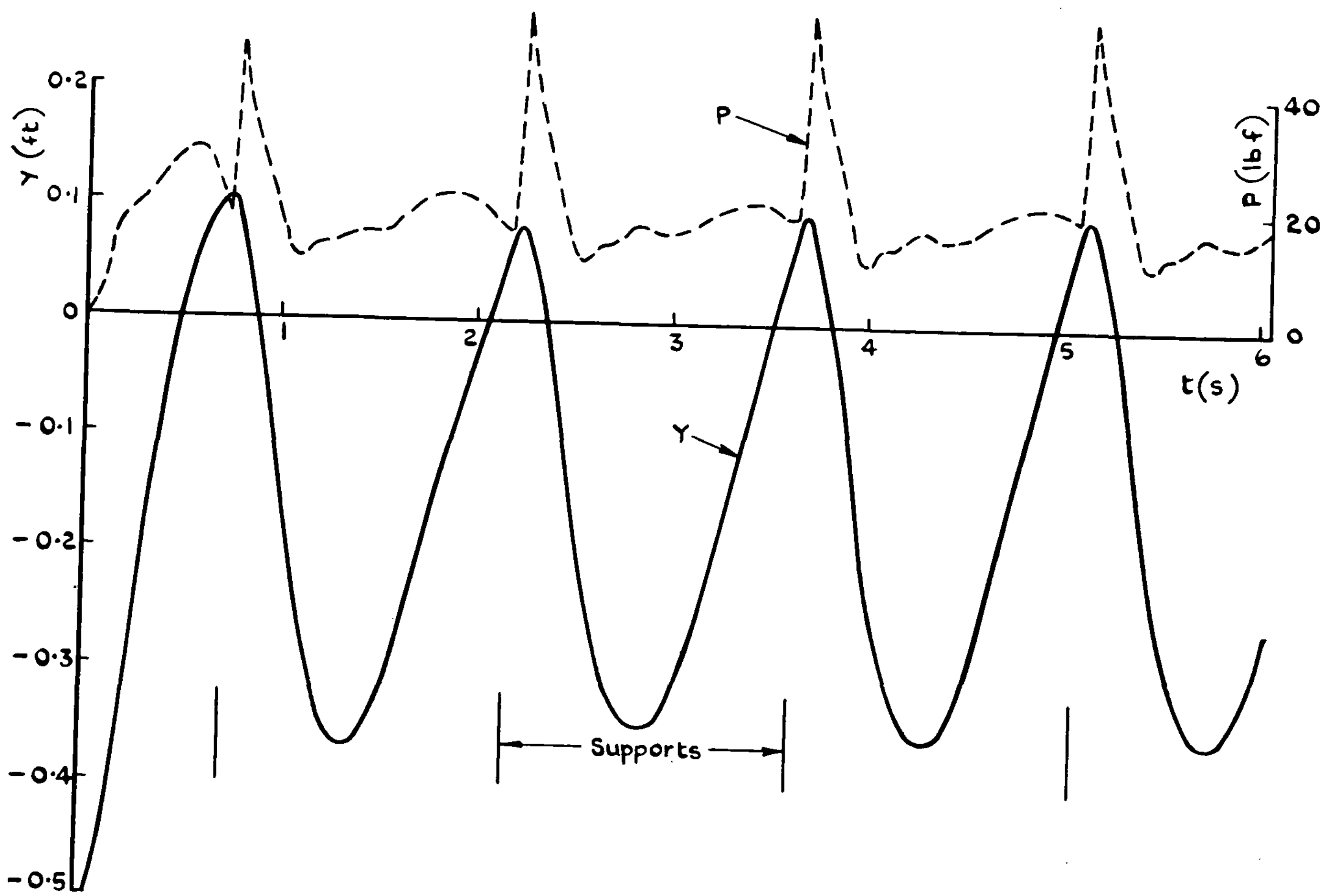

Fig. 4. Numerical results for a trolley wire system

forced oscillation is set up with the selected starting position and initial conditions.

The values of the constants in this example are:

$$\rho = 0\cdot 644 \text{ lb/ft}, \quad EI = 600 \text{ lbf ft}^2,$$
$$T = 4{,}000 \text{ lbf}, \quad \mu = 0\cdot 002 \text{ lbf s/ft},$$
$$S = 240 \text{ lbf/ft}, \quad \lambda = 160 \text{ ft},$$
$$u = 110 \text{ ft/s } (=75 \text{ mile/h}),$$
$$m_1 = 20 \text{ lb}, \quad m_2 = 38 \text{ lb},$$
$$\mu_1 = 9 \text{ lbf s/ft}, \quad \mu_2 = 0\cdot 2 \text{ lbf s/ft},$$
$$k_1 = 560 \text{ lbf/ft}, \quad G = 78 \text{ lbf};$$

using $\Delta x = 3\cdot 33$ ft, $\Delta t = 0\cdot 033$ s.

The numerical method has been extended to examine ways of reducing the peak value of the contact force occurring near the supports. For example, the use of a pantograph comprising three masses instead of two, with a very light head mass. Also, the approximate effect has been computed of smoothing the equilibrium wire profile at the supports by spreaders, and of the use of double springs at the supports separated by a few feet in the along-track direction. It requires only a minor change to the program to include springs at two or more adjacent mesh points, as just the main diagonal of the matrix C has to be changed. Also, a non linear situation has been examined approximately, in which the spring constant S is variable and depends on the local displacement of the wire. Finally, the effect of multiple pantographs can be obtained; this just requires additional trial solutions.

The present more complicated type of overhead system in which the contact wire is suspended by droppers from a catenary wire can be approximated by a related program in which, following Gilbert and Davies (1966), the contact wire is assumed to be suspended from a continuous elastic support of given modulus, which varies with x. The details of the catenary, droppers, main supports, and auxiliary catenary and stitch wires, if any are not included explicitly, but enter implicitly through the value of the modulus of the elastic support, which is a periodic function with wave length equal to the span length to be determined from static tests or a subsidiary calculation. The term $S\Sigma y\delta(x - r\lambda)$ in (1) is now replaced by $S(x)y$ and in the finite difference representation there is a spring force at each pivotal point. Further details of this case are given in Abbott (1967). An example for a simple catenary system is shown in **Fig. 5**.

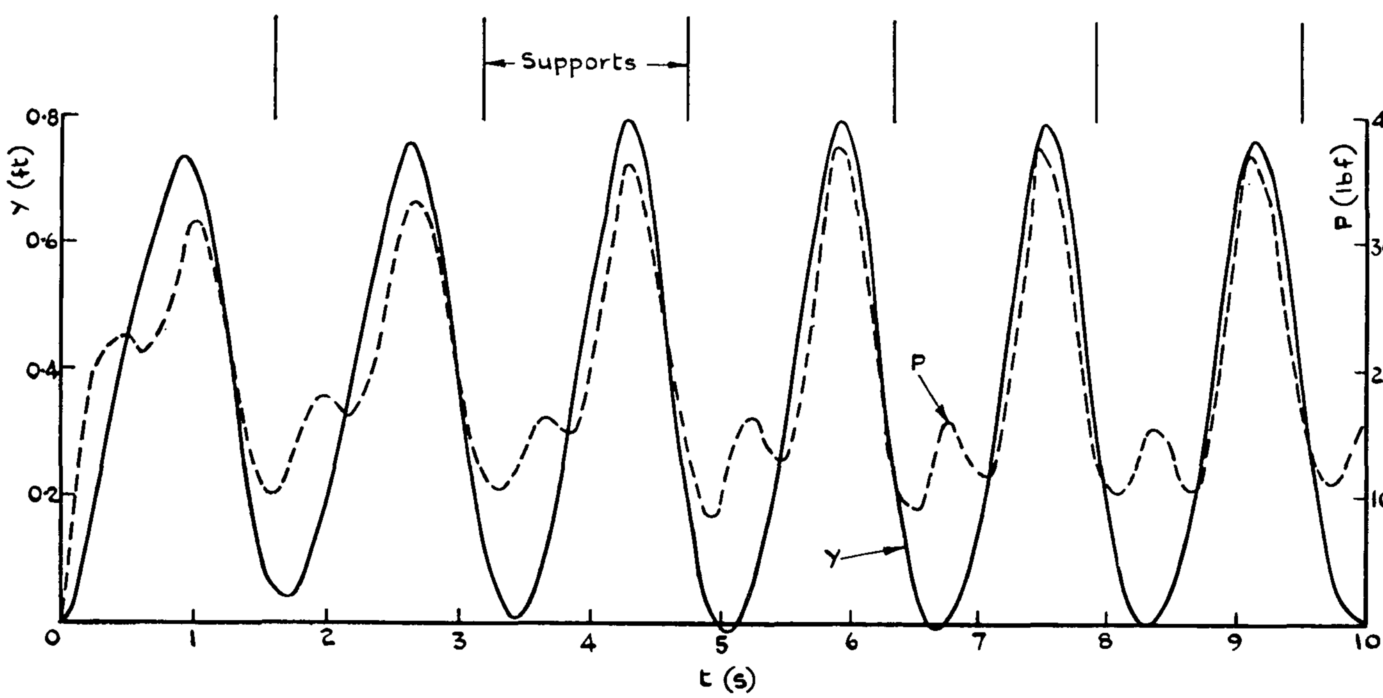

Fig. 5. Numerical results for a catenary system

References

Abbott, M. R. (1967). The numerical solution of a fourth order partial differential equation pertaining to railway overhead contact systems, R. A. E. Technical Report, 67299.

Gilbert, G., and Davies, H. E. H. (1966). Pantograph motion on a nearly uniform railway overhead line, *Proc. IEE*, Vol. 113, No. 3, pp. 485–492.